IEEE Access
The journal for rapid open access publishing
IEEE Xplore Digital Library
http://ieeexplore.ieee.org/Xplore

Application of NMR to test sandstone stress sensitivity of the Dongfang X gas field, China

Qianhua Xiao[1,a], Xinli Zhao[2,a], Wei Lin[2,3], Xiaoliang Huang[1], and Zhangbao Song[1]

Abstract—**The stress sensitivity of reservoir rocks has captured considerable attention in the field of oil and gas development. In this study, nuclear magnetic resonance (NMR) was employed to measure the T2 spectra of sandstone samples from Dongfang X gas field under different confining pressures. According to T2 values, the pores in sandstone samples were divided into macropores (right peak of T2 spectra) and micropores (left peak of T2 spectra), and the stress sensitivity of macropores and micropores were discussed separately. The results show that the increase of net effective stress will lead to the pore deformation of rock samples, and the pore deformation characteristics of rocks in different blocks under different net effective stress can be effectively analyzed by NMR. As the net effective pressure increases, the compression amplitudes of rock samples in different blocks are almost equal, indicating that the reservoirs in the Dongfang X gas field have good homogeneity. Additionally, the study rocks have a weak stress sensitivity, the general stress sensitivity of micropores is stronger than that of macropores. For the samples with high permeability (over 80mD), the compression amplitudes of macropores and micropores are relatively small and close, and the porosity losses are almost the same.**

Index Terms—**Dongfang X gas field, Sandstone, NMR, Stress sensitivity, Macropores and micropores**

I. INTRODUCTION

The stress sensitivity of reservoir rock refers to the phenomenon that the petrophysical parameters (such as porosity, permeability, compression coefficient, etc.) vary with the change of stress state [1]–[4]. For the development of oil and gas reservoirs, the decrease of formation pressure during the primary mining will increase the effective stress of the reservoir, which will further cause the pore compaction of the reservoir rock, leading to the decrease of porosity of the reservoir rock, and at the same time, the permeability of the reservoir rock will also change to some extent [5]–[8]. If the formation pressure decreases greatly, the pore structure of reservoir rock may undergo a certain degree of plastic deformation. Even if the formation pressure recovers in the later water injection (secondary mining), the plastic deformation of microscopic pores and throats cannot be completely restored, and the reservoir permeability will suffer a certain degree of permanent damage [9]–[11]. The compression deformation of the pore structure in rocks caused by the increase of effective stress will not only increase the seepage resistance, but also aggravate other additional effects including Jamin effect [12] and particle migration [13], etc., which will have certain negative effects on the effective development of oil and gas reservoirs. Therefore, the stress sensitivity of reservoir rock is always one of the hot research topics in the field of petroleum industry [14]–[18].

At present, there are mainly two routine methods for testing reservoir sensitivity, one is to analyze reservoir stress sensitivity by increasing confining pressure of cores, and the other is by changing internal pressure and fixing confining pressure of cores [19]–[23]. Fatt and Davis [24] respectively studied the relationship between gas permeability and confining pressure in 8 plunger sandstone samples (permeability ranged from 4.35 to 632 × 10^{-3} um^2) using copper core holder and resin core holder. The experimental results show that the permeability of sandstone samples decreases with the increase of confining pressure, the decrease of permeability mainly occurs in the range of confining pressure less than 21 MPa; when the confining pressure is 21 MPa, the permeability of 8 samples is 59-89% of their permeability without confining pressure; in addition, the permeability under different confining pressures has a function relationship with the overburden confining pressure. Thomas and Ward (1972) [25] found that the stress sensitivity of porosity is weaker than that of permeability in tight gas reservoirs, and the stress has little influence on the effective gas permeability of cores. Walls (1983) [26] has researched into the relationship between rock permeability and stress in tight gas reservoirs, and the relation was found to be nonlinear function; under low stress conditions, the decrease of permeability is greater than that under high stress; the increase of effective stress will make the micro-cracks in the rock closed, and some pores and throats will be compressed until they are completely closed, resulting in the decrease of permeability of rock samples. Davies et al. (1999) [27] systematically compared the permeability stress sensitivity and its influencing factors of unconsolidated turbidites with high porosity and permeability and tight gas reservoirs with low porosity and permeability. The experimental results indicate that for turbidite rocks, the greater the initial porosity and permeability, the stronger the stress sensitivity. Conversely, for tight gas reservoir rocks, the smaller the initial porosity and permeability, the stronger

[1]School of Oil and Gas Engineering, Chongqing University of Science & Technology, Chongqing 401331, P. R. China
[2]Institute of Porous Flow and Fluid Mechanics, University of Chinese Academy of Sciences, Langfang 065007, P.R. China
[3]Department of Earth and Planetary Science, University of California, Berkeley, CA 94720, USA.
Corresponding author: Wei Lin (e-mail: weilin_uc@berkeley.edu; ucaslinwei@126.com).
[a]Qianhua Xiao and Xinli Zhao contributed equally to the paper.
This study was financially supported by the National Science and Technology Project of China [Grant no. 2017ZX05013-001]; the National Natural Science Foundation of China [Grant no. 51604053]; the Chongqing Research Program of Basic Research and Frontier Technology [Grant no. cstc2016jcyjA0126]; the Scientific and Technological Research Program of Chongqing Municipal Education Commission [Grant no. KJ1601313] and National Science Foundation [Grant no. 1724469].
Digital Object Identifier: 10.1109/ACCESS.2019.2928567

the stress sensitivity. It is believed that the difference in micropore geometry accounts for the significant difference in permeability sensitivity between the two rocks. Combined with nuclear magnetic resonance (NMR), scanning electron microscopy (SEM) and conventional flooding experiments, Chen et al. (2001) [28] conducted research on the permeability stress sensitivity characteristics of low permeability siltstone reservoirs in Daqing Oilfield. The magnetic resonance data presents that the right peak amplitude of the T2 spectrum decreased with the increase of the effective stress, while the left peak remained substantially unchanged, reflecting that the larger pores in the rock sample were compressed after the reservoir rock was subjected to the effective stress, while the small pores were not compressed. By simulating the actual reservoir pressure change (that is, constant confining pressure and variable flow pressure), Xiao et al. (2016) [14] conducted permeability stress sensitivity tests on tight clastic sandstone rocks after stress aging, and found that, the stress sensitivity of permeability varies with pore pressure under different confining pressure, and the change of permeability with pore pressure is larger when confining pressure is low, however, the change of permeability with pore pressure is smaller when confining pressure is high. Lin et al. (2008) [29] conducted an experimental study on the stress sensitivity of oil and water single-phase permeability in the ultra-low permeability reservoir of the Yanchang Formation in the Ordos Basin. It is shown that the damage to oil-phase permeability caused by the increase of effective stress is greater than that of water-phase, and the recovery of oil-phase permeability after unloading is less than that of water-phase. Xue et al. (2007) [30] studied the permeability stress sensitivity characteristics of cores with different permeability levels, and revealed that the relative decrease value of permeability of low permeability cores is greater than that of medium and high permeability cores. The stress sensitivity characteristics of permeability can be divided into two types: “gentle type” and “first steep type, then slow type”, and the permeability stress sensitivity of low permeability reservoirs mostly belong to the later.

Rocks are comprised of multiscale pore structures, with dimensions ranging from nano to macroscale [31]–[34]. Previous stress sensitivity studies mainly concentrated in coal and continental sandstone and considered pores of rocks as a whole to analyse the stress sensitivity, the stress sensitivity of different size pores cannot be distinguished. In this study, NMR was used to measure the T2 spectra of marine sandstone samples from Dongfang X gas field under different confining pressures. According to T2 values, the pores in sandstone samples were divided into macropores (right peak of T2 spectra) and micropores (left peak of T2 spectra), and the stress sensitivity of macropores and micropores were discussed separately. It is expected to provide some new ideas for the study of stress sensitivity of marine oil and gas reservoirs.

II. Principle and Method Validation

A. Stress Sensitivity Test Principle Using NMR

The principle of nuclear magnetic resonance (NMR) is the interaction between the nucleus and the magnetic field [35]–[39]. NMR measurements of rocks in saturated water (oil) state actually capture the response signals of fluid hydrogen nuclei in rock pores. Because rocks usually contain different sizes of pores, the spin echo series obtained from NMR measurements of saturated water (oil) rocks are actually the result of the superposition of various transverse relaxation components. The transverse relaxation of fluid in porous media can be described by a relaxation time T2: [40]

$$\frac{1}{T_2} = \frac{1}{T_{2B}} + \rho_2 \frac{S}{V} + \gamma^2 G^2 D \tau^2 / 3 \tag{1}$$

where, $\frac{1}{T_{2B}}$ is the body relaxation term, the magnitude of T_{2B} value depends on the nature of the saturated fluid, 2000∼3000 ms, and its reciprocal is very small, so this item can be removed. $\gamma^2 G^2 D \tau^2 / 3$ is the diffusion relaxation term, D is the diffusion coefficient, G is the inhomogeneity of the internal magnetic field, which is proportional to the external magnetic field, and τ is the echo interval. It can be seen from that $\gamma^2 G^2 D \tau^2 / 3$ the contribution of this item can be neglected, when the external field does not change very strongly (corresponding to G is small) and the echo interval τ is short enough. After removing the first and third items on the right, formula (1) can be approximated as: [41], [42]

$$\frac{1}{T_2} = \rho_2 \frac{S}{V} \tag{2}$$

where, ρ_2 is the surface relaxation intensity, um/ms, depending on the pore surface properties and mineral composition; S/V is the specific surface of a single pore, and $S/V = F_s/r$, F_s is the pore shape factor (dimensionless, for spherical pores, $F_s = 3$, and for cylindrical pores, $F_s = 2$), r is the pore radius, um. Thus, formula (2) can be rewritten as:

$$T_2 = C \cdot r \tag{3}$$

where, $C = \frac{1}{\rho_2 F_s}$ is a constant. Therefore, the T_2 relaxation time reflects the structural characteristics of the flow channel and the strength of the fluid-solid interaction. As can be seen from formula (3), smaller pores have shorter relaxation time and larger pores have longer relaxation time, and pore at various sizes can be distinguished using NMR T2 distributions.

Many documents have demonstrated NMR T2 spectrum can be used to investigate the rock stress sensitivity [43]–[47]. Anovitz and Cole (2015) [44] have concluded that when samples of saturated porous media are measured, the amplitude of the T2 measurement is directly proportional to porosity, and short T2 times generally indicate small pores with large surface-to-volume ratios and low permeability, conversely, longer T2 times indicate larger pores with higher permeability. Li et al. (2019) [45] studied the stress sensitivity of medium- and high volatile bituminous coal based on nuclear magnetic resonance and permeability-porosity tests, and divided the pores of the coal into micro-pores, meso-pores and macro-pores by T2 value. Gao et al. (2019) [47] quantitatively studied on the stress sensitivity of pores in tight sandstone reservoirs of Ordos basin using NMR technique, not only during the compression process, but also during the recovery process of rock samples. Thus, as long as the T2 relaxation times distribution (i.e., T2 spectrum) of saturated water cores under

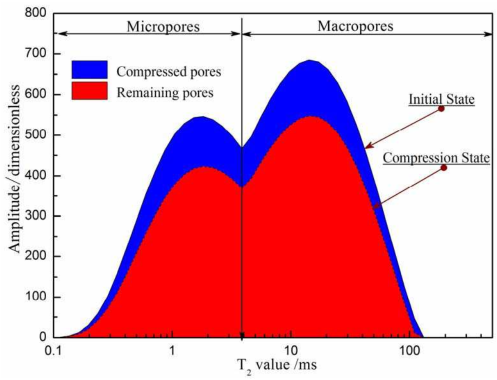

Fig. 1. The T2 spectrum of a rock sample in the District 13 of Dongfang X gas field under different stress states.

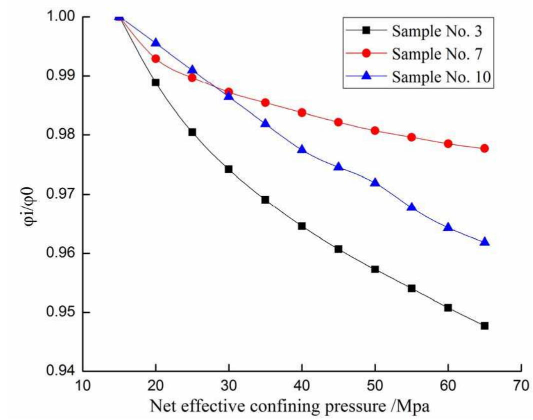

Fig. 2. Results of porosity stress sensitivity of 3 rock samples by routine stress sensitivity experiments.

different stress states is obtained, the variation of pore volume with stress can be quantitatively determined. In this work, we use the loss rate of T2 signal to characterize the sensitivity of pores, termed pseudo porosity loss rate and we call it porosity loss rate in the context. The pseudo porosity loss rate of rock samples under different net confining pressures can be calculated according to the formula (4):

$$\tilde{\phi}_x = \frac{M_0 - M_x}{M_0} \tag{4}$$

where, $\tilde{\phi}_x$ is the pseudo porosity loss rate of rock samples under different net confining pressures, M_0 is the nuclear magnetic T2 signal measured under no confining pressure, M_x is the nuclear magnetic T2 signal measured under different net confining pressures.

B. Method Validation

Fig.1 shows the T2 spectrum of a sandstone sample in the District 13 of Dongfang X gas field under different stress states, different from the T2 spectrum of coal that has triple-peak structure [45], it has a typical bi-modal distribution. Moreover, the T2 signal of rock decreases obviously under the condition of stress, which proves that we can use the loss of T2 value to characterize the stress sensitivity of the study area rock. According to the formula (3) and previous studies [21], [44], [45], [48]–[52], one can acknowledge that smaller pores have shorter relaxation time and larger pores have longer relaxation time, so the area under the left peak can be considered as the content of micropores, while the area below the right peak can be represented as the content of macropores. The difference between the area enclosed by the T2 spectrum in the initial state and that in the compressed state reflects the compression degree of the pores under a certain stress. Hence, the stress sensitivity of the different size of pores can also be analysed by formula (5):

$$\bar{\phi}_x = \frac{M_0^i - M_x^i}{M_0} \tag{5}$$

where, $\bar{\phi}_x$ is the pseudo porosity loss rate of macropores or micropores under different net confining pressures, M_0^i is the nuclear magnetic T2 signal of right peak or left peak measured under no confining pressure, M_x^i is the nuclear magnetic T2 signal of right peak or left peak measured under different net confining pressures, M_0 is the nuclear magnetic T2 signal of double peak measured under no confining pressure.

In order to further verify the accuracy of NMR test for core stress sensitivity of the study reservoir, three representative parallel samples were selected for NMR test and routine stress sensitivity test respectively in this experiment. The detailed information of parallel samples is shown in Table 1. Routine stress sensitivity experiments were carried out on 3 rock samples through variable confining pressure, the experimental results are shown in Fig. 2. In the course of the routine experiments, the internal pressure was kept constant (4 MPa), and the net effective stress on the rock sample was changed by gradually increasing the confining pressure, i.e.,19MPa, 24MPa, 29 MPa, 34 MPa, 39 MPa, 44MPa, 49 MPa, 54 MPa, 59 MPa, 64MPa, 69 MPa, respectively, and the test temperature is 80 °C. The net effective stress is equal to the difference between the confining pressure and the internal pressure. As can be seen from Fig. 2, the porosity damage degree of the rock samples and effective stress satisfy a good power function relationship (R2 > 0.9), the porosity decreases slightly with the increase of effective stress; when the net confining pressure is 20 MPa, the total reduction rate of porosity is about 1%. Meanwhile, comparing the results of routine stress sensitivity test and those of NMR detection of stress sensitivity (Fig. 3), it can be seen that the porosity loss rate measured by both methods shows an increasing trend in the process of increasing confining pressure, and there is good consistency between the two test methods. Therefore, the stress sensitivity test of the research reservoir can be performed by using NMR.

III. Case Application

In this study, 12 typical sandstone samples from 2 blocks and 3 sand bodies in the District 13 of Dongfang X gas field were examined by NMR to investigate the variation characteristics of pore deformation with net effective stress. The basic physical parameters of the selected samples are shown in Table 2, the porosity (ϕ) of the rock samples was measured

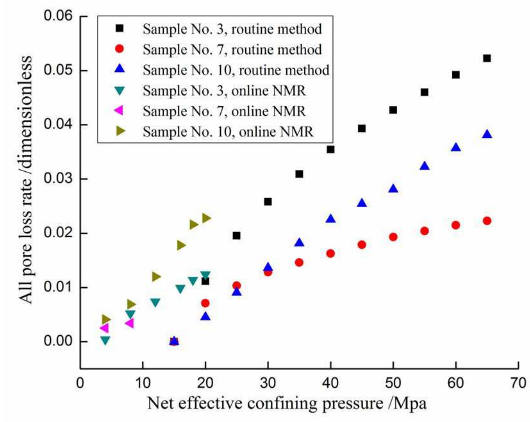

Fig. 3. Comparison of results of routine stress sensitivity tests and NMR tests.

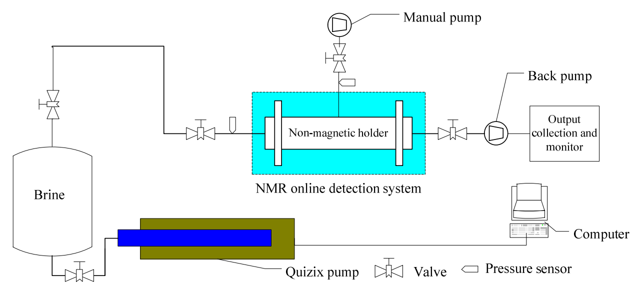

Fig. 4. Schematic diagram of NMR stress sensitivity test.

by the conventional gas measurement using the nitrogen, and the permeability of rock samples (K) was tested according to the requirements of the rock sample Kelvin permeability test industry standard "Core Analysis Method" (SY/T5336-2006). The NMR experiment was carried out on the advanced high temperature and high pressure nuclear magnetic resonance online detection device (MacroMR12-150H-I), and the maximum working temperature and pressure of the equipment can reach 80 °C and 20 MPa respectively. NMR experimental set-up is shown in Fig. 4. NMR test mainly refers to the core analysis method (GBT 29172-2012) and the laboratory measurement specification of nuclear magnetic resonance parameters of rock samples (SY-T6490-2014).

The steps of stress sensitivity detection by NMR are as follows:

1) Sample preparation. First, drill the same size of the plug rock samples, trim the plug faces of the cores; then place the rock samples in a vacuum oven at 85 °C, dry to constant weight; and finally, measure the dry weight (W_1), the length (L) and diameter (D) of the rock samples, calculating the volume of the rock samples (V, $V = \Pi \cdot D^2 \cdot L/4$).

2) Saturation sample with water. The dry rock samples are saturated with simulated formation water whose density is ρ after vacuumed, and the wet weight (W_2) of the rock samples is measured. When the saturated water volume ($(W_2\text{-}W_1)/\rho$) is equal to the pore volume $V \cdot \phi$, it shows that the sample is completely saturated.

3) NMR measurement of rock samples at atmospheric pressure. The rock sample is first vacuumed and second saturated with simulated formation water for 72 hours, then NMR test is carried out under atmospheric pressure.

4) NMR measurement of rock samples at confining pressure.

TABLE I

THE PETROPHYSICAL PARAMETERS OF 3 REPRESENTATIVE PARALLEL SAMPLES. (X DENOTES EFFECTIVE STRESS, Y DENOTES DIMENSIONLESS PERMEABILITY)

Number	Block	Sand body	Bearing Horizon	Porosity /%	Permeability /mD	Relationship between φ_i/φ_0 and stress
3	DF13-1	I	H1 II b	18.180	17.952	$Y=1.1014 x^{-0.036}$, $R^2=0.9994$
7	DF13-2	II	H1 II b	16.880	23.076	$Y=1.0379 x^{-0.014}$, $R^2=0.9843$
10	DF13-2	III	H1 I a	21.340	314.544	$Y=1.0800 x^{-0.027}$, $R^2=0.9822$

TABLE II

THE PETROPHYSICAL PARAMETERS OF 12 SANDSTONE SAMPLES APPLIED FOR NMR MEASUREMENT

Number	Block	Sand body	Bearing Horizon	Depth /m	Porosity /%	Permeability /mD
1	DF13-1	I	H1 II b	2870.20	19.85	14.95
2	DF13-1	I	H1 II b	2868.20	18.48	19.39
3	DF13-1	I	H1 II b	2867.20	18.18	17.95
4	DF13-1	I	H1 II b	2868.30	20.98	21.20
5	DF13-2	II	H1 II b	3136.18	16.35	12.82
6	DF13-2	II	H1 II b	3132.65	15.63	24.25
7	DF13-2	II	H1 II b	3133.96	16.88	23.08
8	DF13-2	II	H1 II b	3130.02	19.32	29.40
9	DF13-2	III	H1 I a	3082.70	18.23	35.06
10	DF13-2	III	H1 I a	3088.55	21.34	314.54
11	DF13-2	III	H1 I a	3087.40	20.26	84.90
12	DF13-2	III	H1 I a	3078.90	22.09	355.72

The NMR test is carried out on the rock sample saturated with simulated formation water under different net confining pressures. The procedure of loading/unloading is as follows, the saturated water sample is placed in the non-magnetic holder, the test temperature is 80 °C, the confining pressure is fixed to 20 MPa by manual pump, and the internal pressure is increased to 20 MPa by Quizix pump. Then the internal pressure is gradually reduced to 16 MPa, 12 MPa, 8 MPa, 4 MPa, 2 Mpa, and 0 MPa, and the corresponding nuclear magnetic T2 signals under different net confining pressures (i.e. 4 MPa, 8 MPa, 12 MPa, 16 MPa, 18 Mpa, and 20 MPa) are measured respectively.

IV. Results and Discussion

The NMR test results of 3 representative rock samples were selected for analysis, as shown in Fig. 5. It can be seen from Fig. 5 that the NMR T2 spectrum of typical samples is a bi-modal distribution, the area under the left peak represents the content of micropores, while the area below the right peak represents the content of macropores. As the permeability of rock samples increases, the left peak of T2 spectrum decreases and the right peak increases. The content of micropores in rock samples no. 1 and no. 5 has little difference from that of macropores (Figs. 5 (a) and 5 (b)), while the content of macropores in rock samples no. 10 is significantly higher than that of micropores (Fig. 5 (c)). Through the T2 spectra tested under the condition of increasing confining pressure, one can find that the T2 spectra of the 3 rock samples shows a decline with the increase of stress.

The increase of the net effective stress will inevitably lead to the deformation of the pores of the rock sample. Comparing the pore deformation characteristics of rocks in two blocks under different net effective stresses (as shown in Fig. 6), we can find that as the net effective stress increases, the compression amplitudes of rock pores are almost equal, indicating that the reservoirs in the Dongfang X gas field have good homogeneity. In addition, with the increase of net effective stress, the amount of pore compressions increases continuously, and the pore is significantly compressed at the initial stage; the greater the increase of net effective confining pressure, the more obvious the compression is; after the net effective confining pressure is increased to 18 MPa, the pores can still be compressed, but the compression amount is slowed down, and finally the pore compression amount gradually becomes constant.

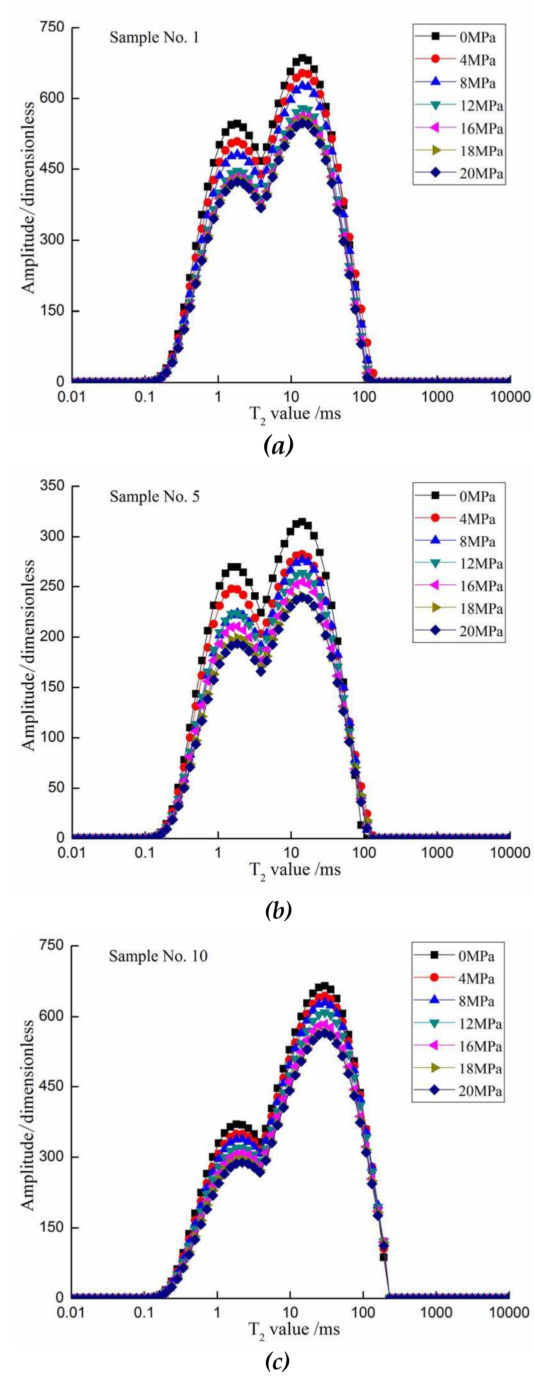

Fig. 5. T2 spectrums of 3 typical rock samples under different net effective stress states.

A. PORE deformation analysis

By means of NMR T2 spectra of rock samples measured under different confining pressures, the variation of pore content with stress can be obtained, Figs 7, 8 were calculated by formula (5) and Fig 9 was calculated by formula (4). Fig. 7 shows the variation characteristics of micropore loss rate with the stress. In the process of increasing the net effective stress from 0MPa to 20MPa, the porosity reduction rate of rocks caused by the stress sensitivity of micropores is as follows: porosity loss rate of sand body I is 0.004-0.019, porosity loss rate of sand body II is 0.004-0.021, porosity loss rate of sand body III is 0.004-0.027, and the porosity loss rate is less than 0.03. The larger the permeability of the sample, the smaller the porosity loss rate of the micropores.

Fig. 8 shows the variation characteristics of porosity loss rate of macropores with the stress. In the process of increasing the net effective stress from 0MPa to 20MPa, the porosity reduction rate of rocks caused by the stress sensitivity of macropores is as follows: porosity loss rate of sand body I is 0.0004-0.0241, porosity loss rate of sand body II is 0.0010-0.0201, porosity loss rate of sand body III is 0.0041-0.0286,

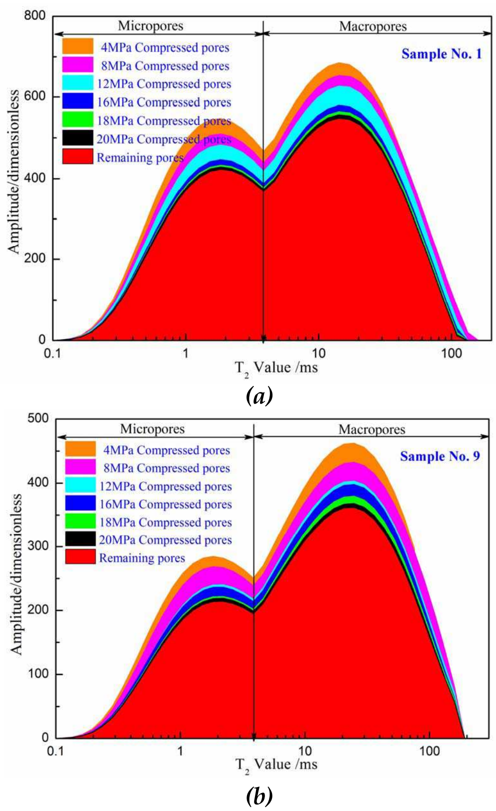

Fig. 6. Comparision of the pore deformation characteristics of rocks in two blocks under different net effective stresses.

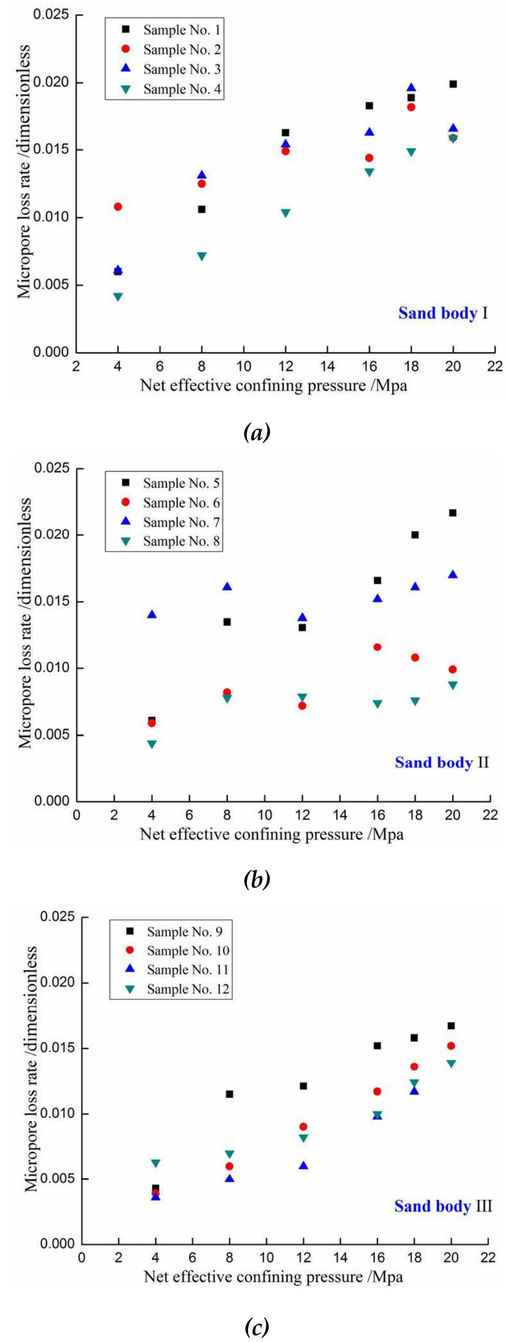

Fig. 7. Variation of micropore loss rate with net effective stress.

and the porosity loss rate is basically less than 0.03. For samples with larger permeability, the macropore loss rate is relatively small. After the permeability exceeds 80mD, the macropore loss rate is relatively close.

Fig. 9 shows the variation characteristics of all pore loss rate with the stress. In the process of increasing the net effective stress from 0MPa to 20MPa, the porosity reduction rate of rocks caused by the stress sensitivity of micropores and macropores is as follows: porosity loss rate of sand body I is 0.006-0.044, porosity loss rate of sand body II is 0.005-0.041, porosity loss rate of sand body III is 0.008-0.039, and the porosity loss rate is basically less than 0.05. For samples with permeability over 80 mD, the all pore loss rate is relatively close and relatively small, which proves that the results of NMR is consistent with that of conventional stress sensitivity test.

B. Stress Sensitivity Analysis OF Micropore and Macropore

By means of NMR T2 spectra of rock samples measured The NMR detection technology can quantitatively distinguish the compression ratio of micropores and macropores under different effective stresses. The compression ratio is defined as:

$$DA = \frac{A_s}{A_{st}} \times 100\% \tag{6}$$

where, A_s is the difference between the area of the left peak (right peak) of T2 spectrum at 0MPa and the area of the left peak (right peak) under certain effective stress; A_{st} is the area enclosed by the left peak (right peak) of T2 spectrum at 0MPa; DA is pore compression ratio, %, which reflects the degree of pore stress sensitivity.

Fig. 10 shows the relationship between compression ratio and effective stress of different sizes of pores of cores with different permeability. It can be seen from Fig. 10 that the smaller the core permeability, the stronger the stress sensitivity of micropores, and the greater the content of micropores (as shown in Fig. 11). Generally, the stress sensitivity of micropores is stronger than that of macropores, which is exactly the opposite of Gao's research [47]. The opposition

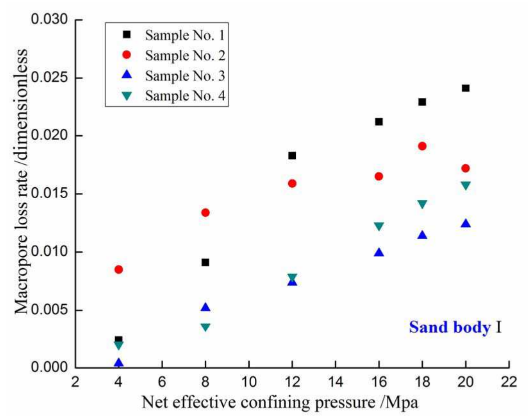

(a)

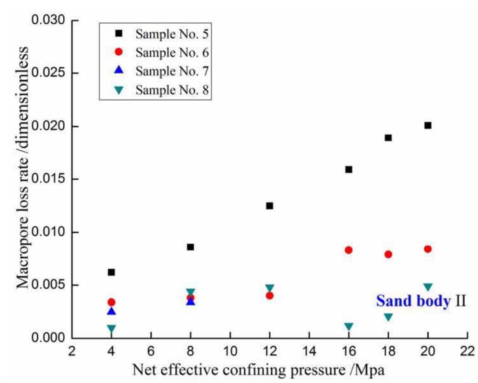

(b)

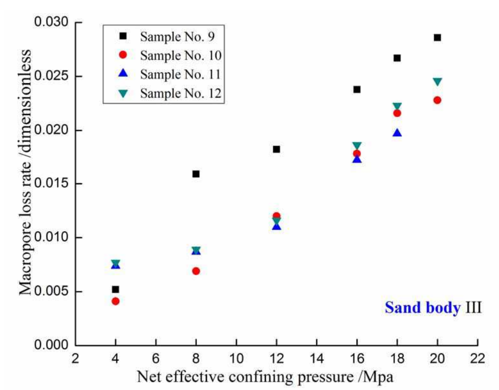

(c)

Fig. 8. Variation of macropore loss rate with net effective stress.

may be due to the different properties of the reservoirs, their study rocks are continental sandstone with low-permeability and low-porosity, and ours are marine high-permeability and high-permeability sandstones. This contrast tells us that even for sandstone reservoirs, the stress sensitivity of rocks is often different because of the different diagenetic environment.

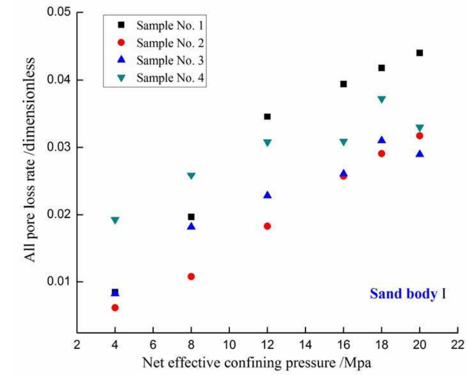

(a)

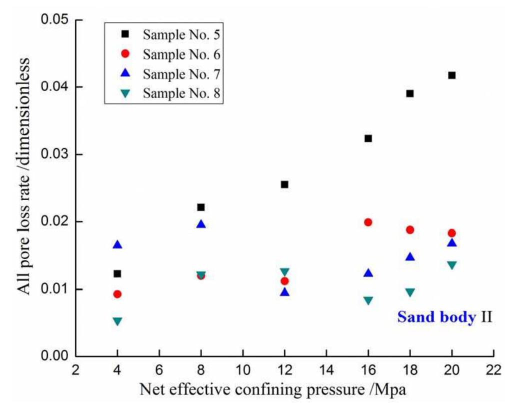

(b)

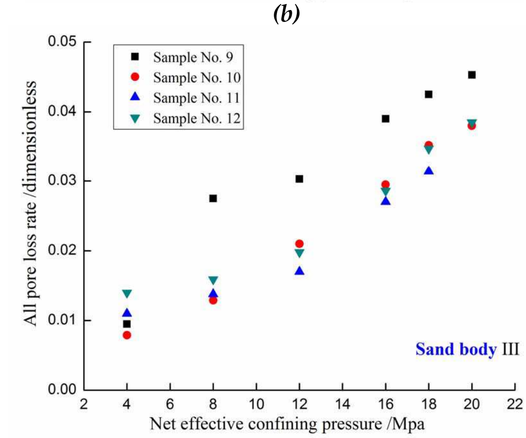

(c)

Fig. 9. Variation of all pore loss rate with net effective stress.

When net effective pressure is less than 6 MPa, the stress sensitivity of micropores of high permeability rock samples is stronger than that of low permeability rock samples. When the net effective pressure is higher than 6 MPa, the stress sensitivity of micropores and macropores of low permeability rock samples is stronger than those of high permeability rock samples.

C. Mechanical Mechanism of Pore Deformation

So far, there are abundant reports on the multi-porosity theory and its application related to the deformation of porous media. For example, Aifantis (1977) [53] introduced the coupling of multi-porosity theory to a deformable porous medium by employing the theory of mixtures, in addition, Wilson and

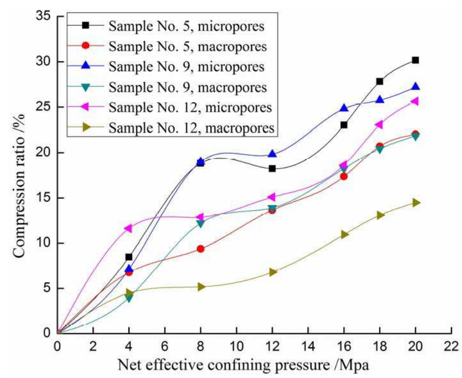

Fig. 10. The relationship between compression ratio and effective stress of different sizes of pores of cores with different permeability.

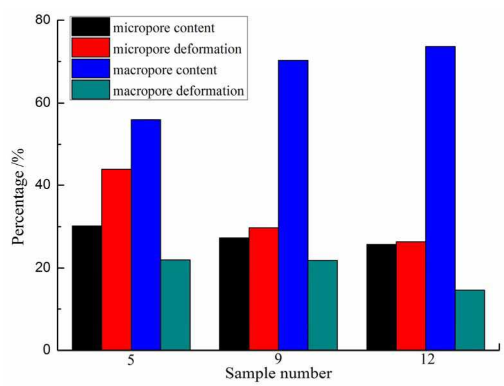

Fig. 11. The characteristics of content and deformation of different size pores in rock samples.

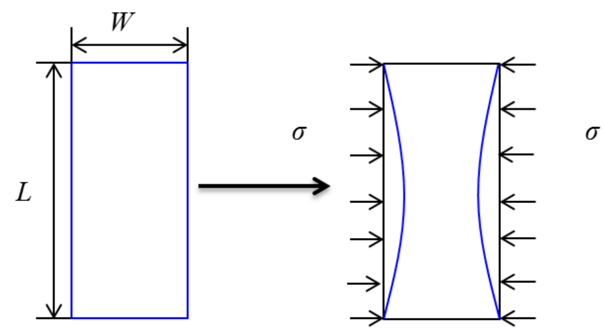

Fig. 12. Schematic diagram of pore cross-section deformation model based on the simply-supported beam model.

Aifantis (1982) [54] presented the theory of consolidation with double porosity. Considering Aifantis' theory of consolidation with double porosity, Svanadze (2005) [55] constructed the fundamental solution of the system of linear partial differential equations of the steady oscillations in terms of elementary functions and determined its basic properties. Based on double porosity theory, Chen and Teufel (2000) [56] conducted model description and comparison study on coupling fluid-flow and geomechanics in dual-porosity modeling of naturally fractured reservoirs, moreover, Shovkun and Espinoza (2017) [57] carried out the coupled fluid flow-geomechanics simulation in stress-sensitive coal and shale reservoirs and analysed the impact of desorption-induced stresses, shear failure, and fines migration.

However, because the T2 spectrums maintain bimodal structure and the induced elastic deformation, here the sandstone samples are single porosity material. In order to explain the experimental results theoretically, a simple bracket bending deformation model in material mechanics [58] was thus adopted to analyse the deformation characteristics of pores of different sizes in sandstone under the same stress. To simplify the theoretical derivation, three assumptions are given:

(1) The sandstone is homogeneous;

(2) The sandstone is elastic and deforms in elasticity;

(3) The cross-section of pores is approximately rectangular.

According to the theory of bending deformation, the deformation of the pore under stress is approximately a combination of bending deformation of two simple brackets, as shown in Fig.12. The following is the bracket deflection equation in material mechanics:

$$q = \frac{\sigma x}{24EI}\left(l^3 - 2lx^2 + x^3\right) \tag{7}$$

where q is the deflection at the distance x from the fulcrum, m; σ is the effective stress acting on the beam, N; E is the elastic modulus of the beam, GPa; I is the inertia distance, m^4; l is the width between the two points, m; x is the distance from one of the pivot points, m.

According to the equation (7), the relationship between the effective stress and the cross-sectional area of the pores can be written [59]:

$$A = WL - 2\int_0^L \frac{\sigma b}{24EI}\left(L^3 - 2Lb^2 + b^3\right) db = WL - \frac{\sigma L^5}{60EI} \tag{8}$$

where A is the pore cross-sectional area, m^2; σ is the effective stress acting on the pore, N; W is the width of the pore cross-section, m; L is the length of the pore cross-section, m; b is the vertical distance of a point on the long side of the fracture section of the pore, m; EI is the bending stiffness of the fracture surface of pores, GPa·m^4, and it is assumed that the sandstone reservoir is a homogeneous body, so it is a fixed value.

The original cross-sectional area of the pore is A_0, m^2, and the cross-sectional area of the elastic deformation of the pore under the stress σ is ΔA, m^2, then the following equation is established:

$$A_0 = WL \tag{9}$$

$$\Delta A = \frac{\sigma L^5}{60EI} \tag{10}$$

Assuming that Ω (dimensionless) is the elastic reduction rate of the cross-sectional area under stress σ, then:

$$\Omega = \frac{\Delta A}{A_0} = \frac{\sigma L^5}{60EIWL} = \frac{\sigma L^4}{60EIW} \tag{11}$$

It can be seen from the Equation (11) that under the same certain stress σ, micro-elastic deformation occurs in pores; based on the bending deformation theory, for a certain length

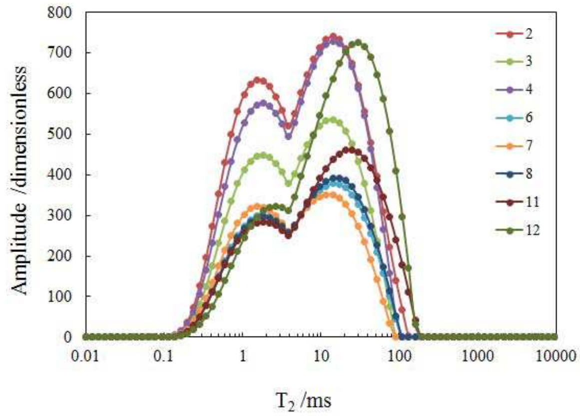

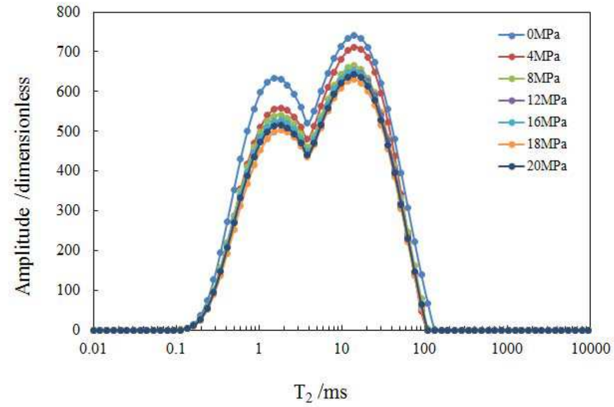

a. Sample 2

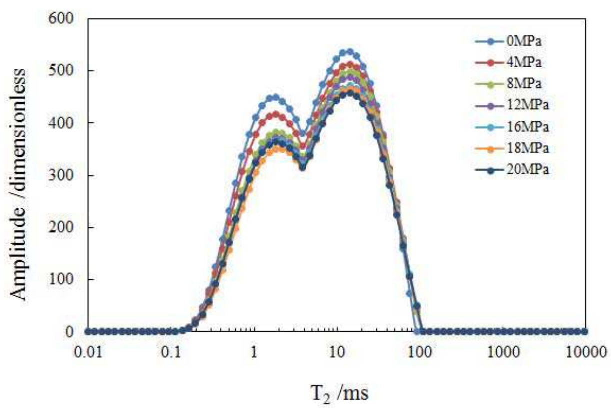

b. Sample 3

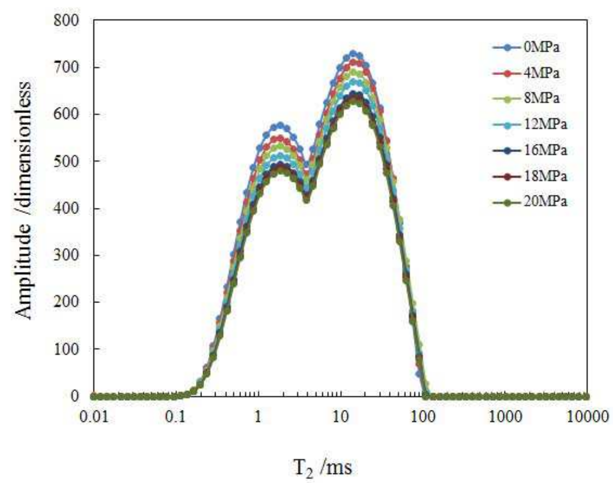

c. Sample 4

Fig. S1. T2 spectrums of the other 8 rock samples without confining pressure.

L, the larger the width W, the smaller the relative damage. This indicates that the relative damage of macropores in the rock is smaller than that of micropores, and coincides with the experimental results.

D. Factors Affecting Stress Sensitivity

Structural deformation and bulk deformation under effective stress are the main reasons for the stress sensitivity of rock, and these two deformations are mainly affected by factors such as rock composition, cement type, rock particle contact mode and pore type. This part mainly analyzes the influence of the above factors on the stress sensitivity of the Dongfang X gas field reservoir.

1) Rock Components: Under the action of external force, the mineral with high hardness is not easy to deform or the deformation is small. The lower the hardness of the mineral, the easier it is to deform. Quartz has the highest hardness in common minerals, followed by feldspar and calcite, and mica and clay minerals have the lowest hardness. Under the external force, the mica and clay minerals with high content of minerals are easily deformed or broken, which reduces the pore volume, and may also cause particle migration to block pores and throats, which will significantly reduce reservoir porosity and permeability. The rock types in the study block are mainly lithic quartz sandstone. The crumb composition is mainly quartz, followed by cuttings, and the feldspar content is the least. The debris composition is complex, and the metamorphic rock cuttings are dominant, followed by a small amount of erupted rock cuttings and muscovite, and no sedimentary rock debris distribution.

2) Cement Type: The cementation determines the stability of the rock particles. Therefore, the different cementing types have an important influence on the reservoir stress sensitivity. From the relationship between the distribution of cement and crumb particles, the stress sensitivity of the clastic cemented rock is the strongest, the pore cementation and contact cementation are the second, and the base cement is the weakest. The core cement in this study area is dominated by carbonate cement such as dolomite, iron dolomite and siderite, followed by a small amount of autogenous clay mineral such as kaolinite. The type of cementation is dominated by pore cementation.

3) Particle Sorting and Contact Relationship: The better the classification of reservoir rock particles, the less likely it is to deform under external force and the weaker the stress sensitivity. The sandstones of the reservoirs in the study

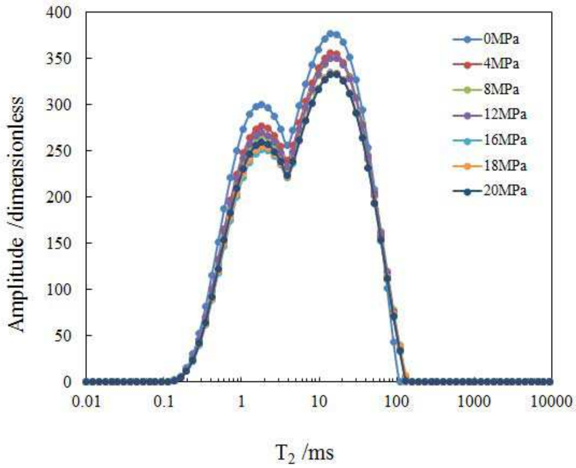

d. Sample 6

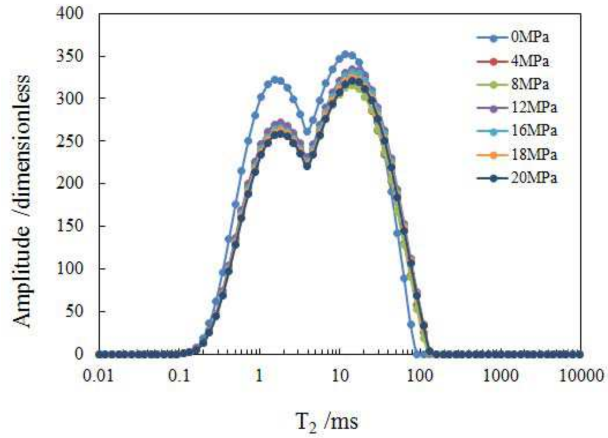

e. Sample 7

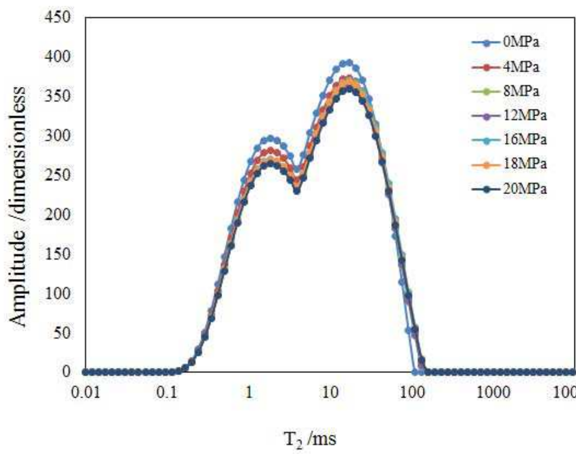

f. Sample 8

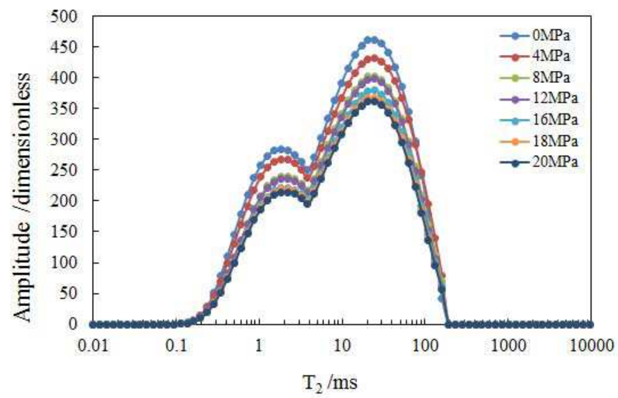

g. Sample 11

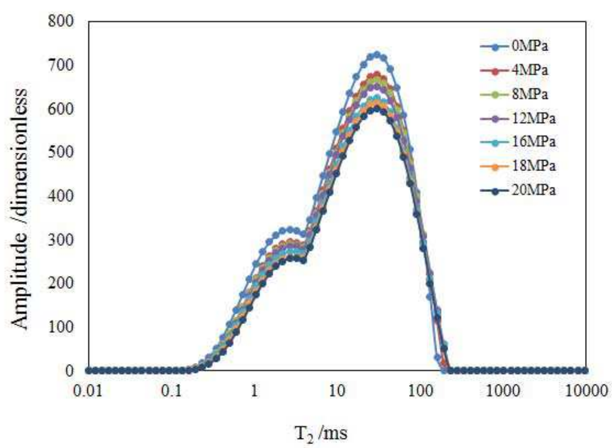

h. Sample 12

Fig. S2. T2 spectrums of the other 8 rock samples under different confining pressure.

block are well-sorted, and the rounding is dominated by sub-edges and sub-circles, and some of them are sub-circle-sub-circular rounding, which is characterized by line-point contact of particle support, followed by spotting, point-line contact, mineral structure maturity is higher.

4) Pore Type: The presence of cracks in the core is the main cause of strong stress sensitivity. The Dongfang X gas field reservoir is mainly composed of intergranular pores and mold pores, followed by intragranular dissolved pores. A small number of biological pores and intercrystalline pores are visible, which are intergranular pore-dissolved pore reservoirs, intergranular pores and molds. The pores are the main reservoir space, and the feldspar and other intragranular dissolved pores and intergranular dissolved pores are the second. In addition, there are also a small amount of pore types such as hetero-micropores, mold pores, and foraminiferal pores. Overall, the main pore combination type is the intergranular pore-molding pore combination type.

As we can see from the analysis, the study rocks are mainly lithic quartz sandstone, well-sorted, and dominated by pore cementation and the intergranular pore-molding pore combination type. This is consistent with the weak stress sensitivity results of the foregoing analysis, and explains that the reservoirs in the Dongfang X gas field have good homogeneity. The difference in stress sensitivity between micropores and macropores may be related to mineral composition and cement type, more direct evidence needs to be observed by energy spectrum or scanning electron microscopy.

V. Conclusions

In conclusion, taking the Dongfang X gas field as the research object, it is proved that NMR can be applied to analyze stress sensitivity of marine reservoir rocks; according to the T2 values, the pores of rocks are divided into macropores and micropores, and the stress sensitivity of macropores and micropores can be further distinguished. In addition, the results indicate that the reservoirs of the Dongfang X gas field have good homogeneity. With the increase of net effective stress, the amount of pore compressions increases continuously, and the pore is significantly compressed at the initial stage; the greater the increase of net effective confining pressure, the more obvious the compression is; after the net effective confining pressure is increased to 18 MPa, the pores can still be compressed, but the compression amount is slowed down, and finally the pore compression amount gradually becomes constant. For the samples with higher permeability, the loss rate of macropores and micropores is relatively small. When the permeability exceeds 80mD, the total porosity loss is close. Generally, the stress sensitivity of micropores is stronger than that of macropores, and the specific mechanism needs to be further revealed.

Acknowledgment

This work was supported in part by China Scholarship Council (CSC), Wei Lin would like to especially recognize Prof. Michael Manga and Dr. Xiaojing Fu for their generous support, guidance and encouragement during his visiting study, and also would like to express the utmost gratitude to Department of Earth and Planetary Science, University of California, Berkley.

Supporting Information

References

[1] Lei, G., Dong, Z.Z., Li, W.R., Wen, Q.Z., Wang, C., 2018. Theoretical study on stress sensitivity of fractal porous media with irreducible water. Fractals-complex Geometry Patterns & Scaling in Nature & Society, 26, 189-199.

[2] Liu, Y.T., Yu, P., Ding, Z.P., 2018. Research on stress-sensitivity of fractured porous media. Journal of Petroleum Science and Engineering, 171, 879-889.

[3] Yin, T.B., Wang, P., Yang, J., Li, X.B., 2018. Mechanical behaviors and damage constitutive model of thermally treated sandstone under impact loading. IEEE ACCESS, 6, 72047-72062.

[4] Zhang, J., Deng, H.W., Deng, J.R., Ke, B., 2018. Development of Energy-Based Brittleness Index for Sandstone Subjected to Freeze-Thaw Cycles and Impact Loads. IEEE ACCESS, 6, 48522-48530.

[5] Smits, R.M.M., de Waal, J.A., van Kooten, J.F.C., 1988. Prediction of abrupt reservoir compaction and surface subsidence caused by pore collapse in carbonates. SPE Formation Evaluation, 3, 340-346.

[6] Dong, P., Lang, Z., Xu, X., 2000. The fully coupled fluid-solid analysis for the reservoir rock deformations due to oil withdrawal. Journal of Geomechanics, 6, 6-10.

[7] Zhang, H., Kang, Y.L., Chen, Y.J., You, L.J., Li, Q.G., 2004. Influence of the rock components and fractures on tight sandstone stress sensitivity. Natural Gas Industry, 24, 55-57.

[8] Cai, Y.Y., Chen, X., Yu, J., Zhou, J.F., 2018. Numerical Study on the Evolution of Mesoscopic Properties and Permeability in Sandstone under Hydromechanical Coupling Conditions Involving Industrial Internet of Things. IEEE ACCESS, 6, 11804-11815.

[9] Li, K.W., Horne, R.N., 2010. Method to evaluate the potential of water injection in naturally fractured reservoirs. Transport in Porous Media, 83, 699-709.

[10] Mehran, S., Masoud, R., Mahmoud, J., Shaun, I., Graeme, R., 2012. Coreflooding studies to investigate the potential of carbonated water injection as an injection strategy for improved oil recovery and co2 storage. Transport in Porous Media, 91, 101-121.

[11] Sun, Z.P., Zhang, H.L., Wei, Z.F., Wang, Y.L., Wu, B.X., Zhuo, S.G., Zhao, Z., Li, J., Hao, L.W., Yang, H., 2018. Effects of slick water fracturing fluid on pore structure and adsorption characteristics of shale reservoir rocks. Journal of Natural Gas Science & Engineering, 51, 27-36.

[12] Li, Z., Qu, Z., 1999. The obvious influence of Jamin effect on lowpermeability reservoirs. Petroleum Exploration & Development, 2, 93-94.

[13] Bahiraei M., 2015. Effect of particle migration on flow and heat transfer characteristics of magnetic nanoparticle suspensions. Journal of Molecular Liquids, 209, 531-538.

[14] Xiao, W.L., Li, T., Li, M., Zhao, J.Z., Zheng, L.L., Li, L., 2016. Evaluation of the stress sensitivity in tight reservoirs. Petroleum Exploration and Development, 43, 115-123.

[15] Ghanimi, M.A., Leroy, Y.M., Kamp, A.M., 2017. Stress-sensitive permeability: application to fault integrity during gas production. Transport in Porous Media, 118, 345-371.

[16] Ouyang, W., Sun, H., Zhang, M., 2018. Well test analysis for multistage fractured horizontal wells in tight gas reservoir considering stress sensitivity. Acta Petrolei Sinica, 39, 570-577.

[17] Zhu, H.Y., Tang, X.H., Liu Q.Y., Liu, S.J., Zhang, B.H., Jiang, S., McLennan, J.D., 2018. Permeability stress-sensitivity in 4D flow-geomechanical coupling of Shouyang CBM reservoir, Qinshui Basin, China. Fuel, 232, 817-832.

[18] Feng, J.W., Dai, J.S., Lu, J.M., Li, X.Z., 2018. Quantitative Prediction of 3-D Multiple Parameters of Tectonic Fractures in Ti Sandstone Reservoirs Based on Geomechanical Method. IEEE ACCESS, 6, 39096-39116.

[19] Nur, A., Byerlee, J.D., 1971. An exact effective stress law for elastic deformation of rock with fluids. Journal of Geophysical Research, 1971, 76, 6414-6419.

[20] Zheng, L.L., Li, M., Zhong, S.q., Xiao, W.L., 2009. Research on calculation of effective stress in low-permeability sandstone rock under cyclic loading and unloading. Acta Petrolei Sinica, 30, 588-592.

[21] Li, S., Tang, D.Z., Pan, Z.J., Xu, H., Huang, W.Q., 2013. Characterization of the stress sensitivity of pores for different rank coals by nuclear magnetic resonance. Fuel, 111, 746-754.

[22] Wang, L., Wang, X.D., 2016. Modelling of pressure transient behaviour for fractured gas wells under stress-sensitive and slippage effects. Int. J. of Oil, Gas and Coal Technology, 11, 18-38.

[23] Zhang, J.J., Wei, C.T., Ju, W., Yan, G.Y., Lu, G.W., Hou, X.W., Kai, Z., 2019. Stress sensitivity characterization and heterogeneous variation of the pore-fracture system in middle-high rank coals reservoir based on NMR experiments. Fuel, 238, 331-344.

[24] Fatt, I., Davis, D.H., 1952. Reduction in permeability with overburden pressure. Journal of Petroleum Technology, 4, 16-16.

[25] Thomas, R.D., Ward, D.C., 1972. Effect of overburden pressure and water saturation on gas permeability of tight sandstone cores. Journal of Petroleum Technology, 24,120-124.

[26] Walls, J.D., 1983. Effects on pore pressure, confining pressure and partial saturation on permeability of sandstones. California£ºStanford University.

[27] Davies, J.P., Davies, D.K., 1999. Stress-Dependent Permeability: Characterization and Modeling. SPE56813, presented at the 1999 SPE annual Technical Conference and Exhibition, Houston, Texas.
[28] Chen, Q., Ye, C.H., Yue, Y., 2001. Investigation of perforation damage characteristics of Berea sandstone by MRI. Magnetic Resonance Imaging, 19, 572-572.
[29] Lin, G.R., Liu, X.G., Lu, Y., Shao, C.G., 2008. Impact of stsess change on percolation pattern of two-phase flow in low permeability reservoir. Special Oil & Gas Reservoirs, 15, 43-45.
[30] Xue, Y.C., Cheng, L.S., 2007. Experimental study on permeability variation with confining pressure in micro-fracture and low-permeability rock. Petroleum Geology & Experiment, 29, 108-110.
[31] You, Q., Wang, H., Zhang, Y., Liu, Y.F., Fang, J.C., Dai, C.L., 2018. Experimental study on spontaneous imbibition of recycled fracturing flow-back fluid to enhance oil recovery in low permeability sandstone reservoirs. Journal of Petroleum Science and Engineering, 166, 375-380.
[32] Lin, W., Li, X.Z., Yang, Z.M., Wang, J., Xiong, S.C., Luo, Y.T., Wu, G.M., 2017. Construction of dual pore 3-D digital cores with a hybrid method combined with physical experiment method and numerical reconstruction method. Transport in porous media, 120, 227-238.
[33] Zhao, X.L., Yang, Z.M., Lin, W., Xiong, S.C., Wei, Y.Y., 2018. Characteristics of microscopic pore-throat structure of tight oil reservoirs in Sichuan Basin measured by rate-controlled mercury injection. Open physics, 16,675-684.
[34] Lin, W., Li, X.Z., Yang, Z.M., Lin, L.J., Xiong, S.C., Wang, Z.Y., Wang, X.Y., Xiao, Q.H., 2018. A new improved threshold segmentation method for scanning images of reservoir rocks considering pore fractal characteristics. Fractals, 26, 1840003.
[35] Dillinger, A., Esteban, L., 2014. Experimental evaluation of reservoir quality in Mesozoic formations of the Perth Basin (Western Australia) by using a laboratory low field Nuclear Magnetic Resonance. Marine and Petroleum Geology, 57, 455-469.
[36] Tyshko, A., Balevicius, S., Padmanaban, S., 2016. An Increase of a Down-Hole Nuclear Magnetic Resonance Tool's Reliability and Accuracy by the Cancellation of a Multi-Module DC/AC Converter's Output's Higher Harmonics. IEEE ACCESS, 4, 7912-7920.
[37] Guo, D., Lu, H.F., Qu, X.B., 2017. A Fast Low Rank Hankel Matrix Factorization Reconstruction Method for Non-Uniformly Sampled Magnetic Resonance Spectroscopy. IEEE ACCESS, 5, 16033-16039.
[38] Ning, Z.P., Zhang, L.X., Lam, J., 2018. Stability and stabilization of a class of stochastic switching systems with lower bound of sojourn time. Automatica, 92, 18-28.
[39] Zhang, P.F., Lu, S.F., Li, J.G., Chen, C., Xue, H.T., Zhang, J., 2018. Petrophysical characterization of oil-bearing shales by low-field nuclear magnetic resonance (NMR). Marine and Petroleum Geology, 89, 775-785.
[40] Timur, A., 1969. Pulsed nuclear magnetic resonance studies of porosity movable fluid and permeability of sandstones. Journal of Petroleum Technology, 21, 775-786.
[41] Kenyon, W.E., 1992. Nuclear magnetic resonance as a petrophysical measurement. Nuclear Geophysics, 6, 153-171.
[42] Kenyon, W.E., 1997. Petrophysical Principles of Applications of NMR Logging. The Log Analyst, 38, 21-43.
[43] Yao, Y.B., Liu, D.M., 2012. Comparison of low-field NMR and mercury intrusion porosimetry in characterizing pore size distributions of coals. Fuel, 95, 152-158.
[44] Anovitz L.M., Cole D.R., 2015. Characterization and Analysis of Porosity and Pore Structures. Reviews in Mineralogy and Geochemistry, 80, 61-164.
[45] Li, X., Fu, X.H., Ranjith, P.G., Xu, J., 2019. Stress sensitivity of medium- and high volatile bituminous coal: An experimental study based on nuclear magnetic resonance and permeability porosity tests. Journal of Petroleum Science and Engineering, 172, 889-910.
[46] Li, A.F., Ren, X.X., Wang, G.J., Wang, Y.Z., Jiang, K.L., 2015. Characterization of pore structure of low permeability reservoirs using a nuclear magnetic resonance method. Journal of China University of Petroleum, 39, 92-98.
[47] Gao, H., Wang, C., Cao, J., He, M.Q., Dou, L.B., 2019. Quantitative study on the stress sensitivity of pores in tight sandstone reservoirs of Ordos basin using NMR technique. Journal of Petroleum Science and Engineering, 172, 401-410.
[48] Wang, W.M., Guo, H.K., Ye, Z.H., 2001. The evaluation of development potential in low permeability oilfield by the aid of NMR movable fluid detecting technology. Acta Petrolei Sinica, 22, 40-44.
[49] Yun, H.Y., Zhao, W.J., Liu, B.K., Zhou, C.C., Zhou, F.M., 2002. Researching Rock Pore Structure with T2 Distribution. Well Logging Technology, 26, 18-21.
[50] Li, H.B., Zhu, J.Y., Guo, H.K., 2008. Methods for Calculating Pore Radius Distribution in Rock from NMR T2 Spectra. Chinese Journal of Magnetic Resonance, 25, 273-280.
[51] Wang, R.F., Shen, P.P., Song, Z.Q., Yang, H., 2009. Characteristics of micro-pore throat in ultra-low permeability sandstone reservoir. Acta Petrolei Sinica, 30, 560-563.
[52] Yang, Z.M., Ma, Z.Z., Luo, Y.T., Zhang, Y.P., Guo, H.K., Lin, W., 2018. A Measured Method for In Situ Viscosity of Fluid in Porous Media by Nuclear Magnetic Resonance. Geofluids, 9542152.
[53] Aifantis, E.C., 1977. Introducing a multi-porous medium. Development Mechanics, 9, 209-211.
[54] Wilson, R.K., and Aifantis, E.C., 1982. On the theory of consolidation with double porosity. International Journal of Engineering Science, 20, 1009-1035.
[55] Svanadze, M., 2005. Fundamental Solution in the Theory of Consolidation with Double Porosity. Journal of the Mechanical Behavior of Materials, 16, 123-130.
[56] Chen, H.Y., and Teufel, W., 2000. Coupling Fluid-Flow and Geomechanics in Dual-Porosity Modeling of Naturally Fractured Reservoirs - Model Description and Comparison. Proceedings of the SPE International Petroleum Conference and Exhibition of Mexico. 10.2118/59043-MS.
[57] Shovkun, I., and Espinoza, D.N., 2017. Coupled fluid flow-geomechanics simulation in stress-sensitive coal and shale reservoirs: Impact of desorption-induced stresses, shear failure, and fines migration. Fuel, 195, 260-272.
[58] Yan, X.P., Wu, H., Yang, L.P., 2013. Material mechanics. Beijing: Tsinghua University Press.
[59] Liu, Y.F., Tang, D.Z., Xu, H., Li, S., Zhao, J.L., Meng, Y.J., 2015. Characteristics of the stress deformation of pore-fracture in coal based on nuclear magnetic resonance. Journal of China Coal Society, 40, 1415-1421

Qianhua Xiao was born in Chongqing, China in 1987. He received the B.S. degree in architecture environment and equipment engineering from Southwest Petroleum University, Chengdu, China, in 2010, and the Ph.D. degree in Fluid Mechanics from Chinese Academy of Sciences, Beijing, China, in 2015.

He is currently an associate Professor and the Director of the Department of Petroleum and Natural Gas Engineering, School of Oil and Gas Engineering, Chongqing University of Science & Technology, Chongqing, China. His research interests include reservoir characteristics analysis, grading evaluation, unconventional oil and gas resource development, and micro- and nanoscale fluid mechanics.

Xinli Zhao was born in Guyuan, Ningxia, China in 1995. He received the B.S. degree in process equipment and control engineering from China University of Petroleum, East China, Qingdao, China, in 2016. He is currently pursuing the Ph.D. degree in fluid mechanics under the supervision of Prof. Zhengming Yang at University of Chinese Academy of Sciences, Beijing, China.

His research focuses on physical simulation and seepage theory of unconventional oil and gas reservoirs. He is currently active in the Society of Petroleum Engineers (SPE), and is serving as the Vice-President of Research Institute of Petroleum Langfang SPE Student Chapter. Some of his research results have been published at premium international journals and conferences, including the Journal of Energy Resources Technology-Transactions of the ASME, International Journal of Oil Gas and Coal Technology, Open Physics, etc. Mr. Zhao's awards and honors include the certificate of participation in the International Petroleum Engineering Professional Challenge (China University of Petroleum, East China), the certificate of Petrowhiz Knowledge Competition (Southwest Petroleum University), and the Pacemaker to Merit Student (University of Chinese Academy of Sciences).

Wei Lin was born in Yibin, Sichuan, China in 1991. He received the B.S. degree in petroleum engineering from China University of Geosciences, Beijing, China, in 2015. He is currently pursuing the Ph.D. degree in fluid mechanics under the supervision of Prof. Xizhe Li and Prof. Zhengming Yang at University of Chinese Academy of Sciences, Beijing, China.

From 2018 to 2019, he started a 12-month visit studying at Department of Earth and Planetary Science, University of California, Berkeley under the supervision of Prof. Michael Manga. His collaborative study is a combination of developing models and percolation theory for tight rocks and volcanic rocks, and performing and analyzing x-ray tomography images of rocks using Advanced Light Source (ALS), Lawrence Berkeley National Laboratory. He is the author of more than 33 articles, and is the first inventor of 4 patents and 1 software. His research expertise and interest includes physical and chemical transport in porous materials, modeling and characterization of porous media, multi-scale matter, tertiary oil recovery including oilfield chemistry and microbial enhanced oil recovery. He was the SPE President of Research Institute of Petroleum Langfang SPE Student Chapter. Since May 2019, he has served as the Bentham Ambassador of Bentham Science Publishers Ltd: Sharjah. He is a reviewer for Marine and Petroleum Geology, Journal of Petroleum Science & Engineering, IEEE Access, Energies, RSC Advances, Journal of Dispersion Science and Technology, Heliyon, International Journal of Mechanics Research, etc.

Mr. Lin's awards and honors include the CAS President Award (Chinese Academy of Sciences, CAS), the Chinese Goverment Scholarship (China Scholarship Council), and the National Scholarship for Doctoral Students (Ministry of Education of the People's Republic of China).

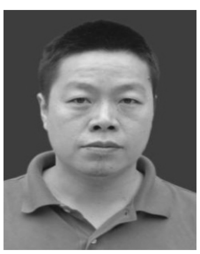

Xiaoliang Huang was born in 1982. He received the B.S. degree in petroleum engineering from Southwest Petroleum University (SWPU), Nanchong, China, in 2005, and the M.S. degree in oil and gas field development engineering from SWPU in 2009.

He is currently an associate Professor of the Department of Petroleum and Natural Gas Engineering, School of Oil and Gas Engineering, Chongqing University of Science & Technology, Chongqing, China. He is the author of one book, more than 40 articles, and one invention. He is mainly engaged in the research of oil and gas seepage theory, oil and gas reservoir engineering and numerical simulation.

Zhangbao Song received the B.S. degree in petroleum and natural gas engineering from Chongqing University of Science & Technology (CQUST), Chongqing, China in 2018. He is currently pursuing the M.S. degree at CQUST. His research interests mainly focus on the development of unconventional oil and gas fields.